LANGMUIR
Article
Cite This: *Langmuir* 2019, 35, 4976−4985
pubs.acs.org/Langmuir

Ionic Strength-Dependent Interactions and Dimensions of Adsorbed Zwitterionic Copolymers

Matthew G. Petroff,[†] Elena A. Garcia,[†] Margarita Herrera-Alonso,*[,‡] and Michael A. Bevan*[,†]

[†]Chemical & Biomolecular Engineering, Johns Hopkins University, Baltimore, Maryland 21218, United States

[‡]Chemical & Biological Engineering & School of Advanced Materials Discovery, Colorado State University, Fort Collins, Colorado 80523, United States

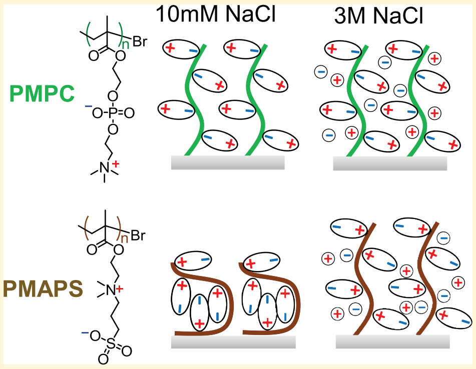

ABSTRACT: We report direct measurements of ionic strength-dependent interactions between different molecular weights of zwitterionic triblock copolymers adsorbed to hydrophobic colloids and surfaces. The zwitterionic copolymers investigated include phosphorylcholine [poly(2-methacryloyloxyethyl phosphorylcholine) (PMPC)] and sulfopropylbetaine [poly(3-(*N*-2-methacryloyloxyethyl-*N*,*N*-dimethyl)ammonatopropanesulfonate) (PMAPS)] end blocks separated by poly(propylene oxide) center blocks. The range of repulsion between adsorbed PMAPS copolymer layers increases with increasing NaCl from 0.01 to 3 M, and layer thicknesses range from ∼50 to 100% of the PMAPS block contour length. In contrast, repulsion between PMPC layers does not change for 0.01−3 M NaCl, and layers remain near full extension at their contour length. NaCl-dependent interactions and inferred layer dimensions correlate with hydrodynamic layer thickness and polymer second virial coefficients. These results suggest that the interaction range and layer thickness of adsorbed zwitterionic copolymers arise from a balance of intramolecular dipolar attraction and repulsion possibly mediated by water solvation. The balance between these competing effects and resulting ionic strength dependence is determined by specific zwitterionic moieties.

■ INTRODUCTION

Zwitterionic polymers have gained recognition as anti-fouling materials[1] with applications in biosensing,[2] drug delivery,[3−6] and filtration.[7−11] Zwitterionic repeat units typically possess side groups containing both a positive quaternary amine and a negative group such as phosphoric acid [phosphorylcholine, poly(2-methacryloyloxyethyl phosphorylcholine (PMPC)], sulfopropyl [sulfobetaine, poly(3-(*N*-2-methacryloyloxyethyl-*N*,*N*-dimethyl)ammonatopropanesulfonate (PMAPS)], or carboxylic acid (carboxybetaine).[12] Charged zwitterionic polymers typically have ionic strength-dependent properties, such as increasing chain dimensions with increasing salt concentration in aqueous media.[13−19] This ionic strength dependence is often referred to as an "anti-polyelectrolyte effect" and has been observed in bulk solution behavior[17,18,20,21] as well as surface architectures of adsorbed or grafted polymers.[13,22] The common explanation is that increasing ionic strength disrupts attractive dipole−dipole interactions between zwitterionic moieties, thus increasing chain dimensions (the opposite behavior observed for conventional polyelectrolytes with repulsive monopole interactions).[17,23] Although zwitterionic polymers have a net neutral charge like poly(ethylene oxide) (PEO), zwitterionic moieties' dipole moments and their ability to be screened by salt can be expected to lead to different chain dimensions and solution phase behavior.

In general, the ionic strength dependence of zwitterionic polymer dimensions is not sufficiently understood for either a priori predictions or a posteriori interpretations of macromolecular properties. For example, computational studies have systematically explored the effects of zwitterionic chemistry on monomer dipole moment and water solvent affinity,[24,25] but findings have not been directly related to macromolecular polymer dimensions or solution behavior. Experimental studies have investigated ionic strength-dependent chain dimensions for different monomer chemistries.[19,20,26,27] For example, different salt-dependent grafted layer thicknesses were observed for sulfobetaines with systematically varied spacer length (i.e., dipole moments) between the positive and negative charge groups.[28] However, dipole moment alone does not sufficiently explain zwitterionic polymer solution behavior. For example, PMPC does not exhibit ionic strength-dependent dimensions in solution or on surfaces,[14,34−36] despite having a similar dipole moment to PMAPS.[29] One explanation is the importance of specific solvation effects, as PMPC analogs with reversed dipole orientations (phosphate−amine to amine−phosphate) displayed ionic strength-dependent dimensions typical of other zwitterionic polymers.[30]

Further understanding of zwitterionic polymer ionic strength-dependent properties may be gained from measures of interactions. For example, static light scattering (SLS)

Received: January 23, 2019
Revised: March 17, 2019
Published: March 20, 2019

DOI: 10.1021/acs.langmuir.9b00218
Langmuir 2019, 35, 4976−4985

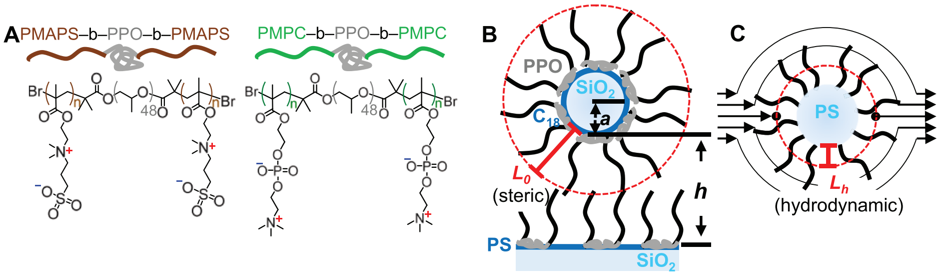

Figure 1. Zwitterionic PMPC and PMAPS triblock copolymers adsorbed onto hydrophobic colloids and surfaces. (A) PMAPS$_n$−PPO$_{48}$−PMAPS$_n$ and PMPC$_n$−PPO$_{48}$−PMPC$_n$ copolymers synthesized in this work. (B) Adsorbed zwitterionic copolymers form dense extended layers from adsorption onto hydrophobic 3 μm colloids and hydrophobic glass slides. The sphere−plane geometry is used to measure interaction potentials using ensemble TIRM.[41] The adsorbed copolymer steric thickness, L_0, corresponds to the distance between the substrate and onset of polymer intermolecular interactions at the layer edge.[38] (C) Dynamic light scattering (DLS) measures adsorbed copolymer hydrodynamic thickness, L_H, on 100 nm hydrophobic colloids, which corresponds to the distance between the substrate and polymer layer edge where liquid does not penetrate.[42]

studies of homopolymer zwitterionic solutions indicate connections between interactions (i.e., second virial coefficients) and chain dimensions (i.e., radius of gyration).[13,18] Findings indicate that PMPC chains have ionic strength-independent dimensions and net repulsive interactions, whereas PMAPS chains display ionic strength-dependent dimensions and interactions from attractive to repulsive (based on second virial coefficients).[31] Measurements of silica surfaces with grafted zwitterionic layers as a function of ionic strength have also been used to infer thicknesses (normal compression) and frictional properties (lateral motion).[14,20] However, while such measurements provide information on zwitterionic layer thicknesses, they do not reveal information about ionic strength-dependent interactions. Finally, measurements of interactions between zwitterionic layers on opposing surfaces have primarily focused on contact adhesion and lubrication.[32−35] However, these studies investigated how ionic strength-dependent electrostatic and dipolar contributions determine net zwitterionic layer intra- and intermolecular interactions relevant to phase behavior of bulk polymers and polymer-coated colloids.[36,37] In particular, prior measurements have not interrogated weak interpenetration and compression at the polymer periphery (i.e., vanishing density profile) that determines net polymer mediated kT-scale interactions.[38]

Our prior study of adsorbed zwitterionic triblock copolymers in fixed physiological ionic strength media demonstrated how intra- and intermolecular interactions between PMPC moieties determined layer dimensions and net interactions.[39] Triblock copolymers with PMPC end blocks of varying molecular weight were ∼2× thicker than polyethylene oxide triblock copolymers of the same degree of polymerization, and PMPC blocks were extended to near their contour length. Aside from differing dimensions between PMPC and PEO, interactions were essentially the same for layers of the same thickness. This suggests that intramolecular dipolar interactions can affect layer dimensions but leave net intermolecular interactions essentially unaffected. Measuring layer dimensions and spatially resolving interaction potentials as a function of ionic strength may help understand how screening of dipolar interactions in different zwitterionic polymers influences their behavior and properties.

In this work, we report measurements of ionic strength-dependent dimensions and interactions of zwitterionic copolymers adsorbed to hydrophobic colloids and surfaces. Measurements are reported for novel zwitterionic copolymers of PMPC−PPO−PMPC and PMAPS−PPO−PMAPS (Figure 1a). As in our prior study of PMPC copolymers at fixed ionic strengths,[39] ensemble total internal reflection microscopy (TIRM)[40] is used to measure kT and nanometer scale interactions, but now between adsorbed copolymers versus ionic strength, pH, and end block molecular weight (Figure 1b). For comparison with measured potentials, light scattering provides complementary measurements of layer hydrodynamic thickness in addition to literature results for unadsorbed zwitterionic homopolymer dimensions and virial coefficients. Our findings show important differences between PMPC and PMAPS copolymer ionic strength-dependent dimensions and interactions, which suggests that specific interactions are important to different zwitterionic copolymers behavior and properties in aqueous media.

■ THEORY

Ensemble TIRM was used to measure particle−surface interactions in this work.[41] In brief, from direct measurement of the colloid's relative height distribution, $P(h)$, the particle-potential energy profile, $U(h)$, is obtained via a Boltzmann relation as

$$\frac{U(h_{\mathrm{i}}) - U_{\mathrm{M}}(h_{\mathrm{M}})}{kT} = \ln\left[\frac{P(h_{\mathrm{i}})}{P(h_{\mathrm{M}})}\right] \tag{1}$$

where "i" and "M" are indices for any height and the most probable height, respectively, k is Boltzmann's constant, and T is absolute temperature. Potential energy profiles are modeled as a superposition of gravitational (G), van der Waals (V), and polymer (P) potentials as[39]

$$U(h) = U_{\mathrm{G}}(h) + U_{\mathrm{V}}(h) + U_{\mathrm{P}}(h) \tag{2}$$

where contributions from electrostatic double layers are negligible in this work (i.e., including them makes no quantitative difference to net potentials) because of the relatively high solution ionic strength (>10 mM) and short Debye lengths ($\kappa^{-1} < 3$ nm) as well as low copolymer-coated colloid surface potentials ($|\zeta| \approx 5$ mV). The gravitational potential energy is given by

$$U_{\mathrm{G}}(h) = \frac{4}{3}\pi a^{3}(\rho_{\mathrm{p}} - \rho_{\mathrm{f}})gh \tag{3}$$

where a is the particle radius, $\rho_{\mathrm{p}} - \rho_{\mathrm{f}}$ is the difference in particle and fluid densities, and g is acceleration due to gravity. The van der Waals and polymer potentials are obtained from flat plate interactions using the Derjaguin approximation to obtain sphere-plate potentials as[43]

$$U(h) = 2\pi a \int_h^{\infty} E(l)\mathrm{d}l \tag{4}$$

where $E(l)$ is the energy per unit area between flat plates at a separation, l, for the interaction of interest. For van der Waals, the interaction between flat plates is given by[43]

$$E(l) = \frac{A_{132}(l)}{12\pi l^2} \tag{5}$$

where A_{132} is the separation-dependent Hamaker function between surfaces of materials 1 and 2 separated by a medium of material 3, which can be computed using the Lifshitz theory and accurately represented for the materials in this work by[44]

$$\begin{aligned} A_{132}(l) &= \frac{1}{2}[1 + 2\kappa l]\exp(-2\kappa l)A_0 + A_{1\infty}(l) \\ A_{1\infty}(l) &= \frac{(a_f + b_f l)}{(1 + c_f l + d_f l^2)} \end{aligned} \tag{6}$$

which includes electrostatic screening via the prefactor including κ^{-1}. The final sphere-plate potential can be reasonably approximated for $h/a > 0.017$ as a power law of the form[45]

$$U_V(h) = 2\pi a \int_h^{\infty} -\frac{A_{132}(l)}{12\pi l^2}\mathrm{d}l \cong -Aah^{-2} \tag{7}$$

For compression of adsorbed polymers between parallel flat plates, the energy per area is[46]

$$\begin{aligned} E(l) &= f_1(l/2) - f_1(L_0) + f_2(l/2) - f_2(L_0) \\ &= 2[f(l/2) - f_0] \end{aligned} \tag{8}$$

where f_0 and L_0 are the uncompressed single polymer layer free energy per area and thickness, and the subscripts refer to polymer layers on surfaces 1 and 2. The free energy per area, $f(L)$, of a flexible polymer brush layer compressed from L_0 to L is[46]

$$f(L) = \frac{5}{9}f_0\left[\frac{L_0}{L} + \left(\frac{L}{L_0}\right)^2 - \frac{1}{5}\left(\frac{L}{L_0}\right)^5\right] \tag{9}$$

which results in a sphere-wall potential for compressing two polymer layers as

$$\begin{aligned} U_P &= 2\pi a \int_h^{2L_0} 2[f(l/2) - f_0]\mathrm{d}l \\ &= \frac{40}{9}\pi a f_0 L_0\left[\ln\left(\frac{2L_0}{h}\right) + \frac{9}{5}\left(\frac{h}{2L_0}\right) - \frac{1}{3}\left(\frac{h}{2L_0}\right)^3 \right. \\ &\qquad \left. + \frac{1}{30}\left(\frac{h}{2L_0}\right)^6 - \frac{47}{30}\right] \end{aligned} \tag{10}$$

which can be well approximated for moderate compression ($L > 0.5L_0$) as[47]

$$U_P(h) \cong 16\pi a(\Gamma/\gamma)f_0 L_0 \exp(-h\gamma/2L_0) \tag{11}$$

where the constants Γ and γ are 10.6 and 7.38, respectively (by fitting eq 11 to 10).

■ MATERIALS AND METHODS

Zwitterionic Copolymer Synthesis. Zwitterionic triblock copolymers were synthesized as PMPC−PPO−PMPC and PMAPS−PPO−PMAPS. Copolymers were synthesized by polymerization of 2-methacryloyloxyethyl phosphorylcholine (MPC) or 3-(*N*-2-methacryloyloxyethyl-*N*,*N*-dimethyl)ammonatopropanesulfonate (MAPS) monomers onto a Br−PPO$_{48}$−Br macroinitiator by activators regenerated by electron transfer−atom transfer radical polymerization using an ascorbic acid reducing agent and CuCl$_2$ catalyst. For PMAPS copolymers, the synthesis procedure was identical to that described in detail in our previous publication,[39] except that it was performed in trifluoroethanol/methanol (75:25 v/v) solvent.

Polymer Characterization. Number averaged molecular weight (M_n) was assessed using ^{1}H NMR recorded on a Bruker AV 400 MHz spectrometer. For PMPC, copolymer spectra was measured in methanol-d_4. M_n was estimated using end group analysis to assess the ratio of PMPC−PPO in the purified product, with results within 10% of that estimated by monomer conversion. For the PMAPS copolymer, NMR spectra of raw and purified PMAPS copolymer was taken in 0.5 M NaCl D$_2$O, and M_n estimated from monomer conversion. For both PMAPS and PMPC copolymers, weight averaged molecular weight (M_w) was estimated using SLS performed with a DAWN HELEOS II (Wyatt Technology) with 658 nm GaAs laser, and 0.05−2.5 mg/mL polymer in trifluoroethanol. M_w was extracted from Zimm plots using the Debye model and Astra 6.1 Software, using refractive index measured by differential refractometry. Polymer properties are summarized in Table 1.

Table 1. Synthesis and Characterization Information of PMPC and PMAPS Copolymers

polymer	M_w/M_n
PMPC$_{57}$-*b*-PPO$_{48}$-*b*-PMPC$_{57}$	1.4
PMPC$_{28}$-*b*-PPO$_{48}$-*b*-PMPC$_{28}$	1.1
PMAPS$_{90}$-*b*-PPO$_{48}$-*b*-PMAPS$_{90}$	1.4
PMAPS$_{29}$-*b*-PPO$_{48}$-*b*-PMAPS$_{29}$	1.3

Colloids and Surfaces. Glass microscope slides (Fisher 12-549-3) were cleaned and rendered hydrophobic by spin-coating (3000 rpm, 1 min) with a 3% w/w solution of polystyrene (Sigma-Aldrich 430102) in toluene (Fisher T324). Silica colloids (3 μm, Bangs Laboratories) were rendered hydrophobic by the addition of the octadecyl ligand as described previously.[47] Polystyrene sulfate latex (120 nm, Thermo Fisher Invitrogen S37391) was used as received. PMPC and PMAPS copolymers were dissolved in the buffer for interaction measurement at 0.5−1 mg/mL, above the fluorometrically measured critical micelle concentration (between 0.01 and 0.05 mg/mL for all copolymers). Adsorbed layers were formed by contacting polymer solutions with hydrophobic colloids or hydrophobic slides for at least of 4 h and rinsing via centrifugation (particles) and washing (slides) with the measurement solution of interest.

Total Internal Reflection Microscopy. Briefly, a 633 nm laser excited an evanescent wave along the NaCl solution−slide interface, with evanescent wave decay lengths of 113.2, 113.67, 125.99, and 126.19 nm for 0.01, 0.15, 1, and 3 M NaCl solutions, respectively. Videos of colloids diffusing in the evanescent wave were captured using a 40× objective (LD Plan-NEOFLUAR) and a 12-bit CCD Camera (Hamamatsu Orca-ER) operating at 4 binning, 4 ms exposure, and 30 ms/frame. Custom software analyzed images to estimate colloid scattering intensity and relative height over time, with interaction potentials determined from eq 1. The gravitational contribution to the net potential was used to fit the colloid radius and subtracted to leave only colloidal−surface interactions as it has a simple linear dependence.[41]

Dynamic Light Scattering. DLS was conducted using a Malvern Instruments Nano-ZS ZetaSizer using a 4 mW He−Ne laser at 633 nm and scattering angle of 173° and measurements at 22 °C. The

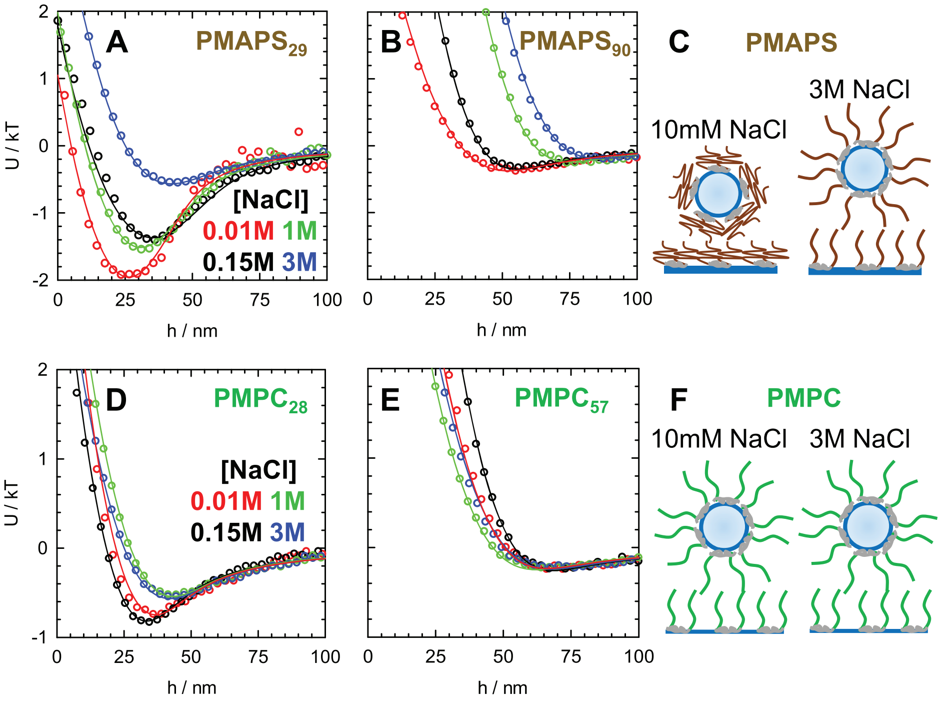

Figure 2. [NaCl]-dependent interactions between zwitterionic copolymers adsorbed to hydrophobic 3 μm colloids and surfaces measured using ensemble TIRM. (A,B) Measured interactions between PMAPS copolymer coated colloids and surfaces (points) with theoretical fits (eq 2) (lines). Legends indicate NaCl concentration and plot titles indicate zwitterionic block repeat units. (C) Schematics depict PMAPS copolymer layer expansion with increasing [NaCl] as indicated by measured potentials. (D,E) Measured interactions between PMPC copolymer coated colloids and surfaces (points) with theoretical fits (eq 2) (lines). (F) Schematics depict PMPC copolymer layer dimensions are invariant to [NaCl] = 0.1−3 M as indicated by measured potentials.

hydrodynamic thickness (L_H) of adsorbed copolymers on colloids was estimated from measurements of coated and bare 120 nm diameter polystyrene particles ($L_H = d_{H,coated} - d_{H,bare})/2$.[42] Hydrodynamic thickness was only reported for monodisperse colloidal dispersions with a polydispersity index (PDI = σ_H^2/d_H^2, with σ_H as the standard deviation in size distribution) less than 0.08.

■ RESULTS AND DISCUSSION

Zwitterionic Copolymer Colloid Stabilization. Figure 1 summarizes the materials and measurement configurations used to investigate ionic strength-dependent interactions of zwitterionic copolymers adsorbed to hydrophobic colloids and surfaces. Amphiphilic PMAPS$_n$−PPO$_{48}$−PMAPS$_n$ and PMPC$_n$−PPO$_{48}$−PMPC$_n$ block copolymers (Figure 1A) were synthesized as described in our previous paper.[39] Previous characterization indicated that copolymers were adsorbed onto hydrophobic colloids and surfaces via poly(propylene oxide) (PPO) blocks and PMAPS and PMPC blocks extending into solution[39] (similar to the well-studied adsorption of PEO-*b*-PPO-*b*-PEO copolymers[48−51]). In the following, we report interactions between adsorbed zwitterionic copolymers adsorbed to hydrophobically modified silica colloids and glass microscope slides (Figure 1B). Results are also reported for light scattering measurements of the hydrodynamic layer thickness of copolymers adsorbed to hydrophobic latex colloids (Figure 1C).

Four copolymers are investigated in this work with average degrees of polymerization per zwitterionic block of n = 28 and 57 for PMPC copolymers and n = 29 and 90 for PMAPS copolymers. The copolymers were all moderately polydisperse with M_w/M_n = 1.1−1.4 (Table 1). The adsorbed PMPC and PMAPS copolymers stabilized colloids against both deposition (on planar substrates) and aggregation (in bulk dispersions) in all NaCl solutions tested in the range of 0.01 to 3 M. Slow deposition and aggregation was observed on ∼24 h time scales after the addition of 1−3 M NaCl solutions. However, this slow destabilization behavior was halted by the addition of 30 ppm polymer. This suggests that the observed instability is likely the result of slow desorption of the zwitterionic copolymers at high ionic strengths (where the zwitterionic end blocks have favorable interactions with the solvent). The additional polymer appears to suppress desorption in a manner consistent with equilibrium adsorption behavior. Notably, the polymer addition was not found to affect the measured potentials of colloids that remained stable; this suggests that surface nonuniformities may have a role in desorption occurring on some particles or surface locations more than others.

Potential Energy Profiles versus Ionic Strength and Block Composition. Potential energy profiles between colloids and surfaces were measured using TIRM as a function of NaCl concentration, end block composition, and end block molecular weight (Figure 2). Interactions were between colloids and surfaces with adsorbed PMAPS (n = 29, 90) and PMPC (n = 28, 57) copolymers at pH 7 in 0.01−3 M NaCl. In all conditions, ensemble average interactions (circles) are well described by fits to eq 2 (lines) (including convolution of theory with a Gaussian kernel to account for finite measurement noise[39]). Because the Hamaker function is known from prior studies,[39,44] and a is independently known from gravitational interactions, the steric thickness, L_0, is the only independent parameter used to fit the colloidal interactions.

DOI: 10.1021/acs.langmuir.9b00218
Langmuir 2019, 35, 4976−4985

NaCl concentration ([NaCl]) significantly influences PMAPS interactions (Figure 2A,B). Increasing [NaCl] causes an increase in the most-probable separation (and corresponding potential energy well location) and a decrease in the attractive well depth. The $PMAPS_{90}$ copolymer interactions occur at larger separations than the $PMAPS_{29}$ copolymer interactions and produce shallower energy wells, which are expected for thicker layers and more repeat units.[52,53] In contrast to the PMAPS copolymer interactions, PMPC copolymer interactions (Figure 2D,E) exhibit a weak [NaCl] dependence. The $PMPC_{57}$ copolymer potentials show little variation across 0.01−3 M NaCl. Except for repulsive decay length variations (unsystematic and within measurement uncertainty), potentials show nearly identical repulsive ranges as well as attractive minimum well depths and separations. The lower molecular weight $PMPC_{28}$ copolymer potentials are also similar for 0.01−3 M NaCl, although with more variation in the repulsive range and attractive well depth. The range variation for $PMPC_{28}$ is also close to measurement uncertainty but may show weak dependence with increasing layer thickness with increasing ionic strength.

The different ionic strength dependencies of the PMAPS and PMPC copolymer layer thicknesses inferred from interactions are consistent with literature results,[14,18,26,27] but the differences between the two polymers are still not obvious. It should be noted that the relatively high ionic strengths cause electrostatic interactions between the charged surfaces to be on shorter ranges than the range of the copolymer interactions. The primary role of [NaCl] is changing the PMAPS layer thickness while leaving the PMPC layer thickness unchanged. While increased screening of attractive dipolar interactions with increasing ionic strength is consistent with the expanding layer thickness for PMAPS (Figure 2C), the ionic strength-independent repulsion, including range and decay length, between PMPC copolymers requires a different explanation.

PMAPS and PMPC copolymer interactions were also measured at different pHs to investigate whether acid−base chemistry had any role in dipolar interactions between zwitterionic moieties. For $PMPC_{28}$- and $PMPC_{57}$-coated colloids, the zeta potential was $\zeta = -2 \pm 4$ mV at pH = 7.2 consistent with net neutral moieties; in contrast, the zeta potential was $\zeta = 8 \pm 5$ mV at pH = 2.5 consistent with protonation of the phosphate group (the monomer $pK_a \approx$ 2.5−3 is reduced to ~1.5−2.0 in polymer and micellar states[54,55]). There was no observable change in PMAPS charge versus pH (from zeta potential), which is expected because the monomer $pK_a < 1$[15,17] is lower than what can be safely measured in our instrument. However, although PMPC showed different zeta potentials, measurements of pH-dependent interactions for both $PMPC_{28}$ and $PMPC_{57}$ copolymers showed no discernible changes from pH = 2.5−7.2. Because changes in zwitterionic dipole moments versus pH do not appear to alter net polymer interactions, this suggests that screening dipolar interactions with increasing ionic strength may also be unimportant for similar reasons.

PMAPS Copolymer Thickness versus [NaCl]. To understand different aspects of the [NaCl]-dependent adsorbed copolymer layer thickness, two measures are reported in this work. (1) The steric thickness (L_0, Figure 1B) corresponds to the onset of repulsion between two opposing adsorbed layers and is obtained by fitting eq 11 to measured potentials. (2) The hydrodynamic thickness (L_H, Figure 1C) corresponds to the equivalent radius of a particle due to excess drag by adsorbed polymer and is obtained by taking the difference in measured hydrodynamic radii of bare and copolymer coated 120 nm polystyrene colloids using DLS.[42] Values of L_0 and L_H can be expected to differ as polymer chains at the adsorbed layer periphery (where the layer density profile vanishes) can have different roles in determining the onset of osmotic compression and the layer permeability to fluid flow.

The thickness of adsorbed PMAPS copolymer layers from both interactions and light scattering is highly dependent on [NaCl]. As shown in Figure 3A, the steric and hydrodynamic thicknesses for $PMAPS_{29}$ and $PMAPS_{90}$ copolymers both increase by ~50% from 0.01 to 3 M NaCl, and $PMAPS_{90}$ is ~3× thicker than $PMAPS_{29}$ at all salt concentrations. Scaling the $PMAPS_{29}$ and $PMAPS_{90}$ thicknesses by the molecular weight-averaged contour length (L_C) of the PMAPS blocks collapses them onto similar curves (Figure 3B).

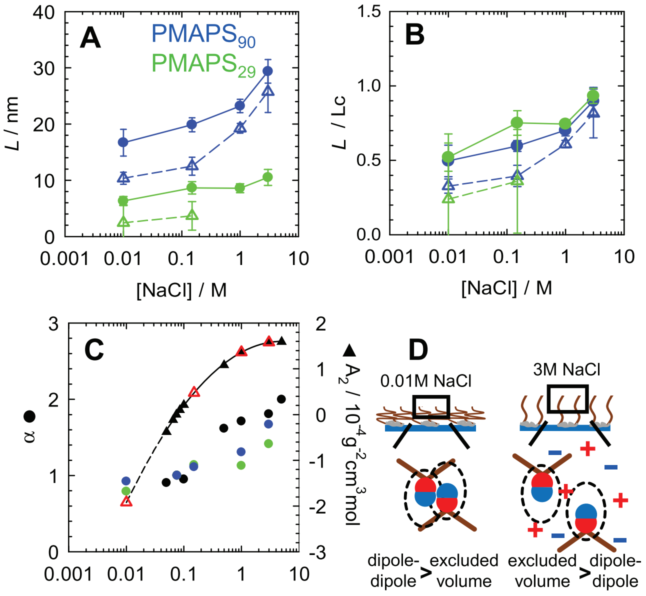

Figure 3. PMAPS copolymer layers are compressed at low [NaCl] and fully extended at high [NaCl]. (A) [NaCl]-dependent thickness of adsorbed $PMAPS_{29}$ and $PMAPS_{90}$ copolymers in terms of the following: (1) steric thickness, L_0 (circles, solid lines; from fits of fit potentials in Figure 2 to eqs 2 (and 11)), (2) hydrodynamic thickness, L_H (triangles, dashed lines) from DLS measurements of bare and coated colloids.[42] (B) Layer thicknesses from panel A scaled by the weight-averaged contour length, L_C, of PMAPS end blocks. (C) [NaCl]-dependent expansion coefficient, α (circles) based on the theta condition at 0.076 M NaCl. Measured L_0 of $PMAPS_{29}$ (green) and $PMAPS_{90}$ (blue) and thickness of grafted $PMAPS_{880}$ (black).[13] [NaCl]-dependent second virial coefficient, A_2 of PMAPS homopolymer. Measurements from Kikuchi et al. (black triangles),[13] fit (black line), and estimated from fit (red triangles). (D) Schematic showing how layer dimensions determined by dominant dipolar attraction at low [NaCl], which is screened at high [NaCl] to yield net repulsive intramolecular interactions.

For [NaCl] = 0.01−3 M, values of L_0 of both PMAPS copolymers extended from $(0.5-0.95)L_C$, whereas L_H were reduced to $(0.25-0.8)L_C$. The reduction of L_H compared to L_0 is greater at low salt concentrations (0.01−0.15 M), which could indicate a low concentration of extended tails leading to longer range steric interactions that remain permeable to fluid flow. Such an architecture is speculative but consistent with

PMAPS density profiles from neutron scattering.[16] The general behavior for $L_0 > L_H$ is consistent with expectations for the increased sensitivity of steric interactions to chains at the polymer layer periphery.[38]

The observation of $L_0 \approx L_C$ at high [NaCl] is unusual for adsorbed polymer layers. Such behavior has been reported in simulations of semiflexible polymers.[56] The kT-scale measurements of steric interactions here can be sensitive to a few highly extended chains at the layer periphery compared to other methods.[38,42] Polydispersity appears to be the most likely explanation for layer thicknesses approaching the end block contour length, where a few large chains can extend beyond the layer periphery.[57,58] Other factors influencing the layer dimensions not accounted for here could include a finite contribution of the PPO blocks or different architecture where the PPO blocks are not attached to the hydrophobic substrates. However, micellar or lamellar structures are not expected because (a) L_0 was similar for adsorption above and below the critical micelle concentration, (b) the measured $L_0 \approx 10-30$ nm is significantly smaller than the ~100 nm micelle dimensions using DLS, and (c) multilayer adsorption is not expected for zwitterionic blocks without addition of polyelectrolytes.[59,60]

The [NaCl]-dependent copolymer layer thickness can also be compared to the relative contraction/expansion of bulk zwitterionic homopolymers from literature studies via an expansion coefficient (Figure 3C). Here, we define an expansion coefficient, $\alpha = (L_0/L_{0,\theta})^{0.5}$. This illustrates the effects of solvent quality on polymer dimensions by normalizing the measured polymer brush dimension (L_0) to the dimension at the theta condition ($L_{0,\theta}$ with a theta condition of 0.076 M NaCl at 298 K for PMAPS[13]). For all PMAPS copolymers, adsorbed layers at 0.01 M NaCl were slightly compressed relative to the theta condition with $\alpha = 0.8-0.9$. At the highest 3 M NaCl concentration, layers were expanded relative to the theta conditions with $\alpha = 1.4-1.7$. For comparison, the thicknesses of much higher molecular weight grafted PMAPS$_{880}$ layers from X-ray scattering have similar α at low ionic strengths but increase to $\alpha = 2$ in 3 M NaCl.[13] In general, the α values are similar versus ionic strength, and the much higher molecular weight PMAPS may be the source of the difference in 3 M NaCl. The PMAPS copolymer expansion follows the general monotonically increasing trend in the second virial coefficient (A_2) versus ionic strength (Figure 3C, with extrapolation below 0.05 M NaCl).[13] This result is consistent with increasing intra- and intermolecular repulsion as layers expand. However, the negative A_2 at 0.01 M NaCl indicating attractive intermolecular interactions is not apparent in the kT-scale potentials measured in Figure 2 at the same ionic strength (only van der Waals attraction between substrates[43,44] is present for these conditions).

The [NaCl] dependence of PMAPS copolymer layer thickness are consistent with "anti-polyelectrolyte" behavior. As is illustrated in Figure 3D, dipolar attraction between zwitterionic moieties dominates at low [NaCl], and then with increasing salt, attraction is balanced by repulsion at the θ condition with $\alpha = 1$. For further increases in [NaCl], dipolar attraction is screened which allows layers to expand in the presence of repulsive solvation and excluded volume effects. The high concentration 3 M NaCl required to reach full layer extension is consistent with ionic strength-mediated screening of dipolar attraction because >1 M NaCl is needed to generate spacing between ions equivalent to the zwitterionic moiety distance along the polymer chains.[20] This extension of the PMAPS brush at high [NaCl] is consistent with an understanding of zwitterionic intermolecular interactions.[18,23]

It is somewhat surprising that the adsorbed PMAPS copolymer layers stabilized colloids for the 2 h of TIRM measurements at the 0.01 M NaCl condition, where attractive intramolecular interactions between copolymer layers on adjacent surfaces could lead to colloidal deposition or aggregation. Notably, for the 0.01 M NaCl condition only, the PMAPS-coated colloids were largely deposited at >24 h of observation as aggregates of >10 particles. This behavior was observed for colloids with both PMAPS copolymer molecular weights, suggesting that the instability was due to attractive interactions between the polymer coatings and not colloidal van der Waals interactions. This result suggests a net kT-scale attraction between PMAPS copolymer layers on adjacent surfaces in 0.01 M NaCl. This attraction may be weaker than expected, as previous measurements report phase separation of PMAPS homopolymer at 0.01 M NaCl.[15] However, these measurements studied much higher molecular weight homopolymers, which would be less tolerant of poor solvent quality than the polymers in our study.[61] Copolymer adsorption to surfaces is also expected to affect chain entropy and solvent quality-dependent phase behavior.[62] Lastly, the A_2 value at 0.01 M NaCl in Figure 3C is uncertain because it was extrapolated from measured data for [NaCl] between 0.5 and 5 M.[13]

PMPC Copolymer Thickness versus [NaCl]. In measurements and plots like those reported for PMAPS copolymer thicknesses, results for the thickness of adsorbed PMPC copolymer layers versus [NaCl] from both interactions (L_0) and light scattering (L_H) are reported in Figure 4 (same format as Figure 3). As shown in Figure 4A, the steric and hydrodynamic thickness for PMPC$_{28}$ and PMPC$_{57}$ copolymers are essentially unchanged from 0.01 to 3 M NaCl. Over the entire [NaCl] range, for adsorbed PMPC$_{28}$ copolymer, $L_0 = 12-14$ nm and $L_H = 10-11$ nm, and for adsorbed PMPC$_{57}$ copolymer, $L_0 = 20-23$ nm and $L_H = 19-22$ nm. For both adsorbed PMPC copolymers, the variation is not correlated with increasing [NaCl] but falls within experimental error. The observed [NaCl] independence of the adsorbed PMPC copolymers is consistent with previous studies of grafted PMPC layers.[16,27]

Scaling the measured PMPC copolymer thicknesses by their molecular weight-averaged contour length (L_C, Figure 4B) collapses all data onto similar curves. For [NaCl] = 0.01−3 M, values of L_0 of both PMPC copolymers extended from $(0.9-1.1)L_C$, whereas L_H values were somewhat smaller at $(0.8-1.0)L_C$. These results indicate that the PMPC brush layers are highly extended, with a significant contribution from higher molecular weight polydisperse chains given dimensions near or slightly greater than the contour length. For both copolymers, $L_0 > L_H$ which is again consistent with expectations based on the sensitivity of steric interactions to a few extended chains at the polymer layer periphery.

The extension of PMPC brushes toward $L_0 \approx L_C$ is somewhat unexpected for typical polymer brush layers. This extension of the PMPC chains is greater than neutron reflectivity studies of grafted PMPC layers reporting extensions of $\sim 0.40L_C$.[16,20] However, these studies investigated grafted PMPC with ~30-fold greater molecular weight and lower adsorbed amounts. All of these differences are expected to lead to higher relative extensions for the PMPC layers in our

DOI: 10.1021/acs.langmuir.9b00218
Langmuir 2019, 35, 4976−4985

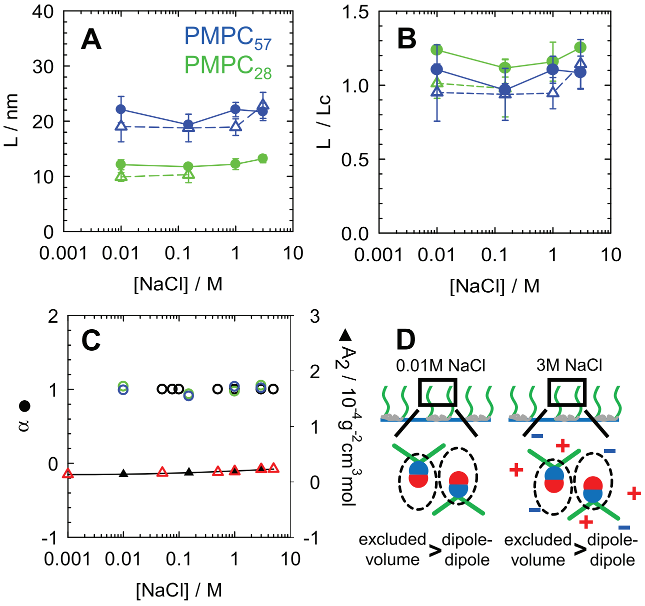

Figure 4. PMPC copolymer layers are highly extended at all [NaCl]. (A) [NaCl]-dependent thickness of adsorbed $PMPC_{28}$ and $PMPC_{57}$ copolymers in terms of the following: (1) steric thickness, L_0 (circles, solid lines; from fits of fit potentials in Figure 2 to eqs 2 (and 11)), (2) hydrodynamic thickness, L_H (triangles, dashed lines) from DLS measurements of bare and coated colloids.[42] (B) Layer thicknesses from panel A scaled by the weight-averaged contour length, L_C, of PMPC end blocks. (C) [NaCl]-dependent expansion coefficient, α (circles), referenced to polymer dimension at 0 M NaCl (because the θ condition not defined). Measured L_0 of $PMPC_{28}$ (green) and $PMPC_{57}$ (blue), and thickness of grafted $PMPC_{790}$[13] (black). [NaCl]-dependent second virial coefficient, A_2 (triangles) of PMPC homopolymer measured by Kikuchi et al. (black triangles),[13] with fit (black line) and estimation from fit (red triangles). (D) Schematic showing extended layers at all [NaCl], indicating net repulsive intramolecular interactions at all conditions.

study.[58,63] As such, the highly extended layers reported here are not necessarily inconsistent with previously reported concentration profiles of grafted PMPC brushes. As discussed in the previous section, adsorption of micelles or multilamellar assemblies are not expected. Again, while determination of PMPC chain molecular weights and polydispersities and finite PPO block thickness may contribute to overestimation of PMPC layer extension, these effects are likely to be small and do not change the conclusions in this work.

The [NaCl] independence of measured PMPC copolymer thicknesses is consistent with PMPC solution properties. For the measured PMPC copolymers, α is essentially unchanged for 0.01−3 M NaCl (Figure 4C) similar to literature results for bulk PMPC homopolymers and grafted PMPC.[13] However, it should be noted that there is no obvious θ condition based on the positive and nearly constant A_2 values from 0 to 5 M NaCl (Figure 4C),[13] so α is referenced to L_0 at 0 M NaCl. PMPC thus exhibits nearly full extension and constant intermolecular repulsion for 0.01−3 M NaCl. As schematically illustrated in Figure 4D, the completely NaCl independent PMPC layer α and A_2 suggest that dipolar attraction is insignificant relative to intramolecular repulsion at all [NaCl].

PMAPS versus PMPC Ionic Strength Dependence. The strong [NaCl] dependence of adsorbed PMAPS copolymer dimensions and [NaCl] independence of adsorbed PMPC copolymer dimensions are consistent with literature studies of bulk and grafted homopolymers characterized with a variety of methods.[13,20] It is interesting to first note that physisorbed triblock copolymers in this work display quantitatively similar [NaCl] dependence to bulk and grafted homopolymers, which is not obvious given the chemical and physical differences of adsorbing copolymers to hydrophobic surfaces (although similar solvent quality dependent behavior is observed for bulk PEO homopolymer and adsorbed PEO triblock copolymers[36−38]). The measured interactions between adsorbed PMAPS and PMPC copolymers in this work show that both polymers generate net intermolecular repulsion at all ionic strengths investigated. Because the interactions are measured with kT-scale resolution in a nonintrusive manner,[64] not unlike light scattering measurements of A_2, the absence of intermolecular attraction is quite clear. In addition, because interactions are spatially resolved on nanometer length scales,[65] it is apparent that attraction is due to substrate van der Waals attraction[43] in comparison to polymer layer interactions.[66]

Although intermolecular interactions are repulsive for both polymers and all [NaCl], intramolecular attractions versus [NaCl] vary for PMAPS but not for PMPC. PMAPS displays intramolecular interactions that vary from net attraction to net repulsion with increasing [NaCl], whereas PMPC displays [NaCl] invariant net repulsion for all conditions tested. The PMAPS ionic strength-dependent behavior is consistent with screening of dipolar attraction between zwitterionic moieties,[18] consistent with models for polyelectrolytes containing positive and negative charges.[23] Such a mechanism is consistent with a net intermolecular repulsion as evident from our potentials (and A_2 measurements), as well as, varying chain dimensions due to [NaCl] dependent intramolecular interactions.

For the PMPC copolymer, the [NaCl] invariant layer dimensions as well as [NaCl] invariant inter- and intramolecular repulsion is not obvious. We are unaware of any study that has uncovered the molecular mechanisms that determine macromolecular properties of PMPC polymers. The backbones of the PMAPS and PMPC copolymers are similar, so the differences in their ionic strength-dependent behavior must be based on their zwitterionic moieties. However, given the balance of all possible combinations of water, dipole, and ion interactions, as well as their solution structures, there are many competing effects to consider that determine net interactions. For example, comparable dipole moments for MPC[29] and MAPS[67] moieties suggest that their screened dipolar attraction should not be significantly different.

In terms of different potential mechanisms for PMPC polymers, simulation[68,69] and spectroscopic[70] studies have suggested that the water structure is unchanged by MPC moieties; this suggests that favorable solvation could produce a net repulsion that stabilizes extended solvated structures at all ionic strengths. In possibly related results from a recent study, [NaCl] sensitivity was recovered for a PMPC analog by switching the orientation of the MPC moiety on the polymer backbone (i.e., swapping amine and phosphate positions);[30] this suggests that the dipole moment is unimportant but could be related to the ability of the repeat unit together with its side group moiety to fit within the water structure. Such an effect is analogous to the aqueous solubility of poly(alkylene oxides), which have no permanent charge or significant dipoles. For example, poly(ethylene oxide) is soluble in water at all concentrations, but poly(propylene oxide) is completely insoluble in water (and at the same time, all alcohol analogues

DOI: 10.1021/acs.langmuir.9b00218
Langmuir 2019, 35, 4976−4985

of the monomers are completely soluble in water).[71] These studies suggest that the water structure on scales comparable to or greater than repeat unit structures, including side groups, is important for chain solubility. Such a description is consistent with spectroscopy measurements that show that the water structure is unchanged by PMPC.[70]

Together, these results show that, depending on the zwitterionic moiety, in addition to screening dipolar attraction, other interactions between ions, dipoles, and water, including structural effects, are necessary to explain macromolecular dimensions and net interactions in different zwitterionic polymers. Our results show on kT energy and nanometer spatial scales how adsorbed layer dimensions and intermolecular interactions depend on [NaCl] for PMPC and PMAPS copolymers adsorbed to hydrophobic substrates. The net intermolecular repulsion between both copolymers at all [NaCl], but different layer thickness dependences on [NaCl], indicate important differences in intramolecular interactions. Future work should identify differences in moiety-dependent intramolecular interactions to develop a comprehensive understanding of zwitterionic polymer properties and behaviors.

■ CONCLUSIONS

Interactions of adsorbed PMPC and PMAPS copolymers were measured as a function of [NaCl] and molecular weight. Novel zwitterionic triblock copolymers of PMPC−PPO−PMPC and PMAPS−PPO−PMAPS were synthesized at several different molecular weights and adsorbed onto hydrophobic surfaces. The resulting high density, extended layers were effective at stabilizing colloids against deposition and aggregation in aqueous 0.1−3 M NaCl media. Measured potential energy profiles show adsorbed PMAPS copolymer layers expand with increasing [NaCl] from 50 to 90% of the end block contour lengths; intermolecular interactions were repulsive at all conditions. In contrast, adsorbed PMPC copolymer layers were extended to near their contour length and displayed intermolecular repulsion at all [NaCl]. The [NaCl]-dependent dimensions of adsorbed triblock copolymers layers when expressed as expansion coefficients are somewhat greater than literature results for PMAPS and PMPC bulk homopolymer and grafted layers, which is explained in terms of polydispersity, adsorbed amounts, and sensitivity to extended chains.

Our findings show how different zwitterionic side groups on similar backbone chain chemistries yield very different behaviors versus [NaCl]. For both PMAPS and PMPC copolymers, our measurements quantify layer thickness with nanometer resolution and intermolecular repulsion with kT-scale sensitivity; this allows us to precisely observe how intramolecular attraction evolves very differently versus [NaCl] for the different zwitterionic moieties. The adsorbed PMAPS copolymer expands with increasing ionic strength in a manner consistent with a mechanism based on screened dipolar attraction. The insensitivity of adsorbed PMPC copolymer dimensions and intermolecular repulsion suggests that intramolecular interactions must have a constant net repulsion that dominates any screened dipolar attraction. Based on our results in combination and literature studies, it seems that water interactions and structuring around MPC moieties may have a critical role in determining the net intramolecular interactions that lead to [NaCl] independent properties. Intramolecular interactions must also simultaneously lead to the highly extended layer architectures observed in both adsorbed PMAPS and PMPC copolymers.

Future work is planned to investigate specific ion effects that influence electrostatic interactions as well as water structure, which may provide some additional insights into the solution behavior of zwitterionic polymers. By measuring zwitterionic intermolecular interactions, our results provide a basis for future studies of zwitterionic−protein interactions and mechanisms associated with their resistance to protein adsorption. Practically, our results demonstrate technologically useful coatings that can be adsorbed to hydrophobic colloids and surfaces to be either dimensionally sensitive or insensitive to NaCl, while retaining repulsive intermolecular interactions.

■ AUTHOR INFORMATION

Corresponding Authors

*E-mail: m.herrera-alonso@colostate.edu (M.H.-A.).
*E-mail: mabevan@jhu.edu (M.A.B.).

ORCID

Michael A. Bevan: 0000-0002-9368-4899

Notes

The authors declare no competing financial interest.

■ ACKNOWLEDGMENTS

We acknowledge financial support by the National Science Foundation (DMR-171067, CMMI-1562639).

■ REFERENCES

(1) Kalasin, S.; Letteri, R. A.; Emrick, T.; Santore, M. M. Adsorbed Polyzwitterion Copolymer Layers Designed for Protein Repellency and Interfacial Retention. *Langmuir* **2017**, *33*, 13708−13717.

(2) Robinson, K. J.; Coffey, J. W.; Muller, D. A.; Young, P. R.; Kendall, M. A. F.; Thurecht, K. J.; Grøndahl, L.; Corrie, S. R. Comparison between Polyethylene Glycol and Zwitterionic Polymers as Antifouling Coatings on Wearable Devices for Selective Antigen Capture from Biological Tissue. *Biointerphases* **2015**, *10*, 04A305.

(3) Shi, S.; Huang, Y.; Chen, X.; Weng, J.; Zheng, N. Optimization of Surface Coating on Small Pd Nanosheets for in Vivo near-Infrared Photothermal Therapy of Tumor. *ACS Appl. Mater. Interfaces* **2015**, *7*, 14369−14375.

(4) Yang, W.; Liu, S.; Bai, T.; Keefe, A. J.; Zhang, L.; Ella-Menye, J.-R.; Li, Y.; Jiang, S. Poly(Carboxybetaine) Nanomaterials Enable Long Circulation and Prevent Polymer-Specific Antibody Production. *Nano Today* **2014**, *9*, 10−16.

(5) Sun, R.; Du, X.-J.; Sun, C.-Y.; Shen, S.; Liu, Y.; Yang, X.-Z.; Bao, Y.; Zhu, Y.-H.; Wang, J. A Block Copolymer of Zwitterionic Polyphosphoester and Polylactic Acid for Drug Delivery. *Biomater. Sci.* **2015**, *3*, 1105−1113.

(6) Sundaram, H. S.; Han, X.; Nowinski, A. K.; Brault, N. D.; Li, Y.; Ella-Menye, J.-R.; Amoaka, K. A.; Cook, K. E.; Marek, P.; Senecal, K.; Jiang, S. Achieving One-Step Surface Coating of Highly Hydrophilic Poly(Carboxybetaine Methacrylate) Polymers on Hydrophobic and Hydrophilic Surfaces. *Adv. Mater. Interfaces* **2014**, *1*, 1400071.

(7) He, M.; Gao, K.; Zhou, L.; Jiao, Z.; Wu, M.; Cao, J.; You, X.; Cai, Z.; Su, Y.; Jiang, Z. Zwitterionic Materials for Antifouling Membrane Surface Construction. *Acta Biomater.* **2016**, *40*, 142−152.

(8) Sun, Q.; Su, Y.; Ma, X.; Wang, Y.; Jiang, Z. Improved Antifouling Property of Zwitterionic Ultrafiltration Membrane Composed of Acrylonitrile and Sulfobetaine Copolymer. *J. Membr. Sci.* **2006**, *285*, 299−305.

(9) Zhao, Y.-F.; Zhu, L.-P.; Yi, Z.; Zhu, B.-K.; Xu, Y.-Y. Improving the Hydrophilicity and Fouling-Resistance of Polysulfone Ultrafiltration Membranes Via Surface Zwitterionicalization Mediated by Polysulfone-Based Triblock Copolymer Additive. *J. Membr. Sci.* **2013**, *440*, 40−47.

DOI: 10.1021/acs.langmuir.9b00218
Langmuir 2019, 35, 4976−4985

(10) Bengani-Lutz, P.; Converse, E.; Cebe, P.; Asatekin, A. Self-Assembling Zwitterionic Copolymers as Membrane Selective Layers with Excellent Fouling Resistance: Effect of Zwitterion Chemistry. *ACS Appl. Mater. Interfaces* **2017**, *9*, 20859−20872.

(11) Lu, R.; Zhang, C.; Piatkovsky, M.; Ulbricht, M.; Herzberg, M.; Nguyen, T. H. Improvement of Virus Removal Using Ultrafiltration Membranes Modified with Grafted Zwitterionic Polymer Hydrogels. *Water Res.* **2017**, *116*, 86−94.

(12) Schlenoff, J. B. Zwitteration: Coating Surfaces with Zwitterionic Functionality to Reduce Nonspecific Adsorption. *Langmuir* **2014**, *30*, 9625−9636.

(13) Kikuchi, M.; Terayama, Y.; Ishikawa, T.; Hoshino, T.; Kobayashi, M.; Ogawa, H.; Masunaga, H.; Koike, J.-i.; Horigome, M.; Ishihara, K.; Takahara, A. Chain Dimension of Polyampholytes in Solution and Immobilized Brush States. *Polym. J.* **2012**, *44*, 121−130.

(14) Higaki, Y.; Fröhlich, B.; Yamamoto, A.; Murakami, R.; Kaneko, M.; Takahara, A.; Tanaka, M. Ion-Specific Modulation of Interfacial Interaction Potentials between Solid Substrates and Cell-Sized Particles Mediated Via Zwitterionic, Super-Hydrophilic Poly-(Sulfobetaine) Brushes. *J. Phys. Chem. B* **2017**, *121*, 1396−1404.

(15) Weers, J. G.; Rathman, J. F.; Axe, F. U.; Crichlow, C. A.; Foland, L. D.; Scheuing, D. R.; Wiersema, R. J.; Zielske, A. G. Effect of the Intramolecular Charge Separation Distance on the Solution Properties of Betaines and Sulfobetaines. *Langmuir* **1991**, *7*, 854−867.

(16) Kobayashi, M.; Ishihara, K.; Takahara, A. Neutron Reflectivity Study of the Swollen Structure of Polyzwitterion and Polyeletrolyte Brushes in Aqueous Solution. *J. Biomater. Sci., Polym. Ed.* **2014**, *25*, 1673−1686.

(17) Mary, P.; Bendejacq, D. D.; Labeau, M.-P.; Dupuis, P. Reconciling Low- and High-Salt Solution Behavior of Sulfobetaine Polyzwitterions. *J. Phys. Chem. B* **2007**, *111*, 7767−7777.

(18) Kikuchi, M.; Terayama, Y.; Ishikawa, T.; Hoshino, T.; Kobayashi, M.; Ohta, N.; Jinnai, H.; Takahara, A. Salt Dependence of the Chain Stiffness and Excluded-Volume Strength for the Polymethacrylate-Type Sulfopropylbetaine in Aqueous Nacl Solutions. *Macromolecules* **2015**, *48*, 7194−7204.

(19) Yang, J.; Chen, H.; Xiao, S.; Shen, M.; Chen, F.; Fan, P.; Zhong, M.; Zheng, J. Salt-Responsive Zwitterionic Polymer Brushes with Tunable Friction and Antifouling Properties. *Langmuir* **2015**, *31*, 9125−9133.

(20) Kobayashi, M.; Terayama, Y.; Kikuchi, M.; Takahara, A. Chain Dimensions and Surface Characterization of Superhydrophilic Polymer Brushes with Zwitterion Side Groups. *Soft Matter* **2013**, *9*, 5138.

(21) Kato, T.; Takahashi, A. Excluded Volume Effects of Sulphobetaine Polymers. *Ber. Bunenges. Phys. Chem.* **1996**, *100*, 784−787.

(22) Dong, Z.; Mao, J.; Yang, M.; Wang, D.; Bo, S.; Ji, X. Phase Behavior of Poly(Sulfobetaine Methacrylate)-Grafted Silica Nanoparticles and Their Stability in Protein Solutions. *Langmuir* **2011**, *27*, 15282−15291.

(23) Higgs, P. G.; Joanny, J. F. Theory of Polyampholyte Solutions. *J. Chem. Phys.* **1991**, *94*, 1543−1554.

(24) Shao, Q.; Jiang, S. Influence of Charged Groups on the Properties of Zwitterionic Moieties: A Molecular Simulation Study. *J. Phys. Chem. B* **2014**, *118*, 7630−7637.

(25) Shao, Q.; He, Y.; Jiang, S. Molecular Dynamics Simulation Study of Ion Interactions with Zwitterions. *J. Phys. Chem. B* **2011**, *115*, 8358−8363.

(26) Leng, C.; Han, X.; Shao, Q.; Zhu, Y.; Li, Y.; Jiang, S.; Chen, Z. In Situ Probing of the Surface Hydration of Zwitterionic Polymer Brushes: Structural and Environmental Effects. *J. Phys. Chem. C* **2014**, *118*, 15840−15845.

(27) Zhang, Z.; Moxey, M.; Alswieleh, A.; Morse, A. J.; Lewis, A. L.; Geoghegan, M.; Leggett, G. J. Effect of Salt on Phosphorylcholine-Based Zwitterionic Polymer Brushes. *Langmuir* **2016**, *32*, 5048−5057.

(28) Higaki, Y.; Inutsuka, Y.; Sakamaki, T.; Terayama, Y.; Takenaka, A.; Higaki, K.; Yamada, N. L.; Moriwaki, T.; Ikemoto, Y.; Takahara, A. Effect of Charged Group Spacer Length on Hydration State in Zwitterionic Poly(Sulfobetaine) Brushes. *Langmuir* **2017**, *33*, 8404−8412.

(29) Mashaghi, A.; Partovi-Azar, P.; Jadidi, T.; Nafari, N.; Maass, P.; Tabar, M. R. R.; Bonn, M.; Bakker, H. J. Hydration Strongly Affects the Molecular and Electronic Structure of Membrane Phospholipids. *J. Chem. Phys.* **2012**, *136*, 114709.

(30) Morozova, S.; Hu, G.; Emrick, T.; Muthukumar, M. Influence of Dipole Orientation on Solution Properties of Polyzwitterions. *ACS Macro Lett.* **2016**, *5*, 118−122.

(31) Terayama, Y.; Arita, H.; Ishikawa, T.; Kikuchi, M.; Mitamura, K.; Kobayashi, M.; Yamada, N. L.; Takahara, A. Chain Dimensions in Free and Immobilized Brush States of Polysulfobetaine in Aqueous Solution at Various Salt Concentrations. *J. Phys.: Conf. Ser.* **2011**, *272*, 012010.

(32) Chen, M.; Briscoe, W. H.; Armes, S. P.; Klein, J. Lubrication at Physiological Pressures by Polyzwitterionic Brushes. *Science* **2009**, *323*, 1698−1701.

(33) Iuster, N.; Tairy, O.; Driver, M. J.; Armes, S. P.; Klein, J. Cross-Linking Highly Lubricious Phosphocholinated Polymer Brushes: Effect on Surface Interactions and Frictional Behavior. *Macromolecules* **2017**, *50*, 7361−7371.

(34) Zhang, L.; Cao, Z.; Bai, T.; Carr, L.; Ella-Menye, J.-R.; Irvin, C.; Ratner, B. D.; Jiang, S. Zwitterionic Hydrogels Implanted in Mice Resist the Foreign-Body Reaction. *Nat. Biotechnol.* **2013**, *31*, 553.

(35) Musoke, M.; Luckham, P. F. Solvent Quality Dependent Interactions between Adsorbed Block Copolymers Measured by Afm. *Colloids Surf., A* **2009**, *337*, 1−8.

(36) Bevan, M. A.; Prieve, D. C. Effect of Physisorbed Polymers on the Interaction of Latex Particles and Their Dispersion Stability. In *Polymers in Particulate Systems: Properties and Applications*; Hackley, V. A., Somasundran, P., Lewis, J. A., Eds.; Marcel Dekker: New York, 2001.

(37) Bevan, M. A.; Petris, S. N.; Chan, D. Y. C. Solvent Quality Dependent Continuum Van Der Waals Attraction and Phase Behavior for Colloids Bearing Nonuniform Adsorbed Polymer Layers. *Langmuir* **2002**, *18*, 7845−7852.

(38) Bevan, M. A.; Prieve, D. C. Forces and Hydrodynamic Interactions between Polystyrene Surfaces with Adsorbed PEO−PPO−PEO. *Langmuir* **2000**, *16*, 9274−9281.

(39) Petroff, M. G.; Garcia, E. A.; Dengler, R. A.; Herrera-Alonso, M.; Bevan, M. A. Kt-Scale Interactions and Stability of Colloids with Adsorbed Zwitterionic and Ethylene Oxide Copolymers. *Macromolecules* **2018**, *51*, 9156−9164.

(40) Wu, H.-J.; Pangburn, T. O.; Beckham, R. E.; Bevan, M. A. Measurement and Interpretation of Particle−Particle and Particle−Wall Interactions in Levitated Colloidal Ensembles. *Langmuir* **2005**, *21*, 9879−9888.

(41) Wu, H.-J.; Bevan, M. A. Direct Measurement of Single and Ensemble Average Particle−Surface Potential Energy Profiles. *Langmuir* **2005**, *21*, 1244−1254.

(42) Min, G. K.; Bevan, M. A.; Prieve, D. C.; Patterson, G. D. Light scattering characterization of polystyrene latex with and without adsorbed polymer. *Colloids Surf., A* **2002**, *202*, 9−21.

(43) Bevan, M. A.; Prieve, D. C. Direct Measurement of Retarded Van Der Waals Attraction. *Langmuir* **1999**, *15*, 7925−7936.

(44) Bitter, J. L.; Duncan, G. A.; Beltran-Villegas, D. J.; Fairbrother, D. H.; Bevan, M. A. Anomalous Silica Colloid Stability and Gel Layer Mediated Interactions. *Langmuir* **2013**, *29*, 8835.

(45) Wu, H.-J.; Everett, W. N.; Anekal, S. G.; Bevan, M. A. Mapping Patterned Potential Energy Landscapes with Diffusing Colloidal Probes. *Langmuir* **2006**, *22*, 6826−6836.

(46) Milner, S. T. Compressing Polymer "Brushes": a Quantitative Comparison of Theory and Experiment. *Europhys. Lett.* **1988**, *7*, 695−699.

(47) Eichmann, S. L.; Meric, G.; Swavola, J. C.; Bevan, M. A. Diffusing Colloidal Probes of Protein-Carbohydrate Interactions. *Langmuir* **2013**, *29*, 2299−2310.

(48) Baker, J. A.; Berg, J. C. Investigation of the adsorption configuration of polyethylene oxide and its copolymers with

polypropylene oxide on model polystyrene latex dispersions. *Langmuir* **1988**, *4*, 1055−1061.

(49) Brandani, P.; Stroeve, P. Adsorption and Desorption of Peo - Ppo - Peo Triblock Copolymers on a Self-Assembled Hydrophobic Surface. *Macromolecules* **2003**, *36*, 9492−9501.

(50) Alexandridis, P.; Alan Hatton, T. Poly(Ethylene Oxide)-Poly(Propylene Oxide)-Poly(Ethylene Oxide) Block Copolymer Surfactants in Aqueous Solutions and at Interfaces: Thermodynamics, Structure, Dynamics, and Modeling. *Colloids Surf., A* **1995**, *96*, 1−46.

(51) Nejadnik, M. R.; Olsson, A. L. J.; Sharma, P. K.; van der Mei, H. C.; Norde, W.; Busscher, H. J. Adsorption of Pluronic F-127 on Surfaces with Different Hydrophobicities Probed by Quartz Crystal Microbalance with Dissipation. *Langmuir* **2009**, *25*, 6245−6249.

(52) Milner, S. T.; Witten, T. A.; Cates, M. E. Theory of the grafted polymer brush. *Macromolecules* **1988**, *21*, 2610−2619.

(53) Milner, S. T. Polymer Brushes. *Science* **1991**, *251*, 905−914.

(54) Marsh, D. *Handbook of Lipid Bilayers*; CRC Press, 2013.

(55) Laschewsky, A. Structures and Synthesis of Zwitterionic Polymers. *Polymers* **2014**, *6*, 1544−1601.

(56) Egorov, S. A.; Hsu, H.-p.; Milchev, A.; Binder, K. Semiflexible polymer brushes and the brush-mushroom crossover. *Soft Matter* **2015**, *11*, 2604−2616.

(57) Milner, S. T.; Witten, T. A.; Cates, M. E. Effects of Polydispersity in the End-Grafted Polymer Brush. *Macromolecules* **1989**, *22*, 853−861.

(58) de Vos, W. M.; Leermakers, F. A. M. Modeling the Structure of a Polydisperse Polymer Brush. *Polymer* **2009**, *50*, 305−316.

(59) Kharlampieva, E.; Izumrudov, V. A.; Sukhishvili, S. A. Electrostatic Layer-by-Layer Self-Assembly of Poly(Carboxybetaine)-S: Role of Zwitterions in Film Growth. *Macromolecules* **2007**, *40*, 3663−3668.

(60) Salloum, D. S.; Olenych, S. G.; Keller, T. C. S.; Schlenoff, J. B. Vascular Smooth Muscle Cells on Polyelectrolyte Multilayers: Hydrophobicity-Directed Adhesion and Growth. *Biomacromolecules* **2005**, *6*, 161−167.

(61) Rubinstein, M.; Colby, R. H. *Polymer Physics*; Oxford University Press: New York, 2003.

(62) Zhulina, E. B.; Borisov, O. V.; Pryamitsyn, V. A.; Birshtein, T. M. Coil-Globule Type Transitions in Polymers. 1. Collapse of Layers of Grafted Polymer Chains. *Macromolecules* **1991**, *24*, 140.

(63) Egorov, S. A.; Hsu, H.-p.; Milchev, A.; Binder, K. Semiflexible polymer brushes and the brush-mushroom crossover. *Soft Matter* **2015**, *11*, 2604−2616.

(64) Bevan, M. A.; Eichmann, S. L. Optical Microscopy Measurements of Kt-Scale Colloidal Interactions. *Curr. Opin. Colloid Interface Sci.* **2011**, *16*, 149−157.

(65) Prieve, D. C. Measurement of Colloidal Forces with Tirm. *Adv. Colloid Interface Sci.* **1999**, *82*, 93−125.

(66) Dagastine, R.; Bevan, M.; White, L.; Prieve, D. Calculation of Van Der Waals Forces with Diffuse Coatings: Applications to Roughness and Adsorbed Polymers. *J. Adhesion* **2004**, *80*, 365−394.

(67) Mathis, A.; Zheng, Y.-L.; Galin, J. C. Random Ethylacrylate Zwitterionic Copolymers: 3. Microphase Separation as a Function of the Zwitterion Structure. *Polymer* **1991**, *32*, 3080−3085.

(68) Ishihara, K.; Mu, M.; Konno, T.; Inoue, Y.; Fukazawa, K. The Unique Hydration State of Poly(2-Methacryloyloxyethyl Phosphorylcholine). *J. Biomater. Sci., Polym. Ed.* **2017**, *28*, 884−899.

(69) Shao, Q.; Jiang, S. Molecular Understanding and Design of Zwitterionic Materials. *Chem. Eng.* **2015**, *27*, 15.

(70) Kitano, H.; Sudo, K.; Ichikawa, K.; Ide, M.; Ishihara, K. Raman Spectroscopic Study on the Structure of Water in Aqueous Polyelectrolyte Solutions. *J. Phys. Chem. B* **2000**, *104*, 11425−11429.

(71) Kjellander, R.; Florin, E. Water Structure and Changes in Thermal Stability of the System Poly(Ethylene Oxide)-Water. *J. Chem. Soc., Faraday Trans. I* **1981**, *77*, 2053−2077.

DOI: 10.1021/acs.langmuir.9b00218
Langmuir 2019, 35, 4976−4985